J. Phycol. **44,** 803–813 (2008)

DOI: 10.1111/j.1529-8817.2008.00509.x

RATE OF O_2 PRODUCTION DERIVED FROM PULSE-AMPLITUDE-MODULATED FLUORESCENCE: TESTING THREE BIOOPTICAL APPROACHES AGAINST MEASURED O_2-PRODUCTION RATE[1]

Torunn B. Hancke,[2] *Kasper Hancke, Geir Johnsen, and Egil Sakshaug*

Department of Biology, Trondhjem Biological Station, Norwegian University of Science and Technology, N-7491 Trondheim, Norway

Light absorption by phytoplankton is both species specific and affected by photoacclimational status. To estimate oxygenic photosynthesis from pulse-amplitude-modulated (PAM) fluorescence, the amount of quanta absorbed by PSII needs to be quantified. We present here three different biooptical approaches to estimate the fraction of light absorbed by PSII: (1) the factor 0.5, which implies that absorbed light is equally distributed among PSI and PSII; (2) the fraction of chl *a* in PSII, determined as the ratio between the scaled red-peak fluorescence excitation and the red absorption peak; and (3) the measure of light absorbed by PSII, determined from the scaling of the fluorescence excitation spectra to the absorption spectra by the "no-overshoot" procedure. Three marine phytoplankton species were used as test organisms: *Prorocentrum minimum* (Pavill.) J. Schiller (Dinophyceae), *Prymnesium parvum* cf. *patelliferum* (J. C. Green, D. J. Hibberd et Pienaar) A. Larsen (Haptophyceae), and *Phaeodactylum tricornutum* Bohlin (Bacillariophyceae). Photosynthesis versus irradiance (*P* vs. *E*) parameters calculated using the three approaches were compared with *P* versus *E* parameters obtained from simultaneously measured rates of oxygen production. Generally, approach 1 underestimated, while approach 2 overestimated the gross O_2-production rate calculated from PAM fluorescence. Approach 3, in principle the best approach to estimate quanta absorbed by PSII, was also superior according to observations. Hence, we recommend approach 3 for estimation of gross O_2-production rates based on PAM fluorescence measurements.

Key index words: **biooptics; chl *a* fluorescence; PAM; photosynthetic oxygen production; PSII-scaled fluorescence excitation**

Abbreviations: **AQ_{PSII}, absorbed quanta by PSII; *E*, irradiance; ETR, electron transfer rate; LHC, light-harvesting complexes associated with PSI and PSII; *P*, photosynthesis; PAM, pulse amplitude modulated; Q_A, quinone A; QR, quantum requirement; RC, reaction centers in PSI or PSII; rETR, relative electron transfer rate**

In the past decades, there has been a growing worldwide demand for efficiently measuring and monitoring primary production of phytoplankton. Traditionally, photosynthesis in aquatic systems is measured as carbon fixation using the ^{14}C method (Steemann-Nielsen 1952). This method, however, is labor intensive, and the quantum yield of carbon fixation varies according to changes in the rate constants for the intermediate steps in photosynthesis, variability in environmental conditions, and the growth phase of the cells (Kroon et al. 1993). As a consequence, models of primary production based on the ^{14}C method are inaccurate (Prézelin et al. 1991, Falkowski and Woodhead 1992, Kroon et al. 1993, Schofield et al. 1993).

PAM fluorescence in combination with biooptical measurements offers a technique to estimate the gross photosynthetic oxygen-production rate. The technique, which is based on in vivo variable fluorescence, estimates the photochemical efficiency of PSII (Schreiber et al. 1986); it is fast and noninvasive and provides information on chl *a* fluorescence kinetics (Govindjee 1995). The quantum yield of charge separation in PSII (Φ_{PSII}), which can be calculated (Genty et al. 1989), depends on the redox state of the first stable electron acceptor in PSII (Q_A). When all the Q_A are oxidized in dark-acclimated cells, the reaction centers (RCs) are open, photochemistry can proceed, and fluorescence emission is low. When all Q_A are reduced under actinic light, the RCs are closed, and photosynthesis is saturated. The energy that hits a closed RC is dissipated as heat and fluorescence emission (Owens 1991).

Using the PAM technique, dark-acclimated cells are excited with a red probe light that is not sufficient enough to induce photosynthesis, ensuring that the detected fluorescence is derived only from the light-harvesting antenna pigments. The initial fluorescence (F_0) can be measured only in dark-acclimated cells, which possess the maximum fraction of open RCs. To determine the maximum fluorescence (F_m), a saturation pulse of white light is applied to the dark-acclimated cells in order to close all RCs in PSII. The pulse induces a primary stable charge separation of the first electron (e^-) acceptor of PSII (Q_A). Measured under actinic light, the initial and maximum fluorescence are denoted F_0' and F_m', respectively. Kroon et al.

[1]Received 15 December 2006. Accepted 21 September 2007.
[2]Author for correspondence: e-mail torunn.hancke@bio.ntnu.no.

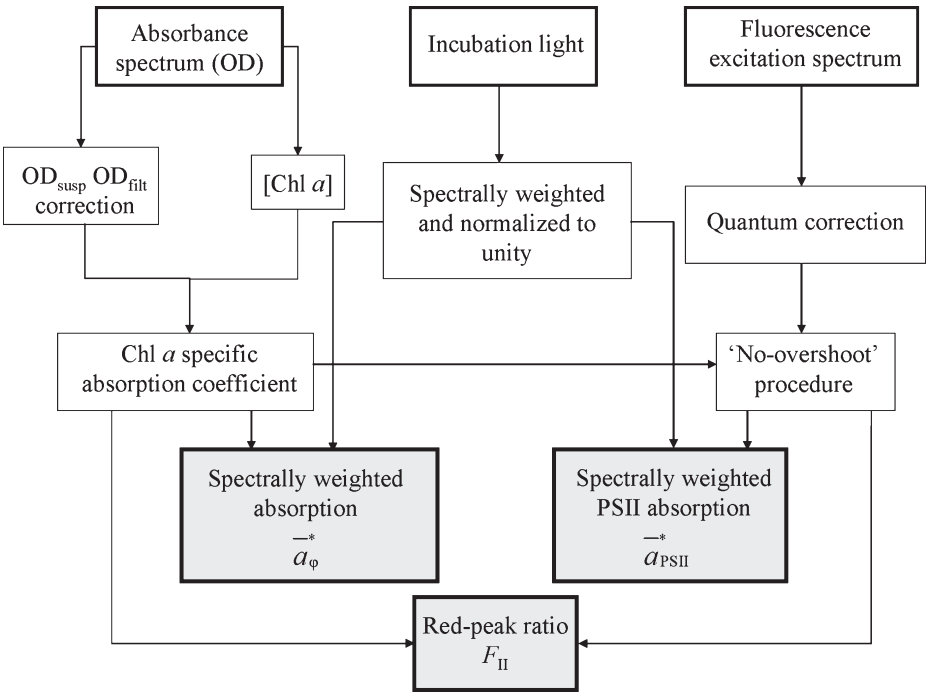

FIG. 1. Schematic drawing of the steps involved in the biooptical determination of the fraction of light absorbed by PSII according to Johnsen and Sakshaug (1996) and Johnsen et al. (1997). The incubation light source is given in PAR, 400–700 nm. F_{II} and $\overline{a}^{*}_{PSII}$ are evaluated as new input parameters to estimate light absorbed by PSII using pulse-amplitude-modulated fluorometry to estimate oxygenic photosynthesis.

(1993) modeled the oxygen-production rate (P_{PSII}) by quantifying the relationship between light absorbed by PSII (AQ_{PSII}), the quantum yield of charge separation in PSII (Φ_{PSII}), and the stoichiometric ratio of oxygen evolved per electron generated in PSII (Γ). To estimate AQ_{PSII}, biooptical measurements are required. The in vivo chl *a*–specific absorption coefficient [$a^{*}_{\phi}(\lambda)$, $m^2(mg\ chl\ a)^{-1}$] (Morel et al. 1987) yields information on total absorption of photosynthetic and photoprotective pigments and reflects the photoacclimation status of the phytoplankton (Johnsen and Sakshaug 1993). The in vivo fluorescence excitation spectrum represents the fraction of light received by PSII (Haxo 1985, Neori et al. 1988). If scaled to $a^{*}_{\phi}(\lambda)$ by the ''no-overshoot'' procedure described by Johnsen et al. (1997), assuming 100% conversion efficiency at the wavelength of maximum fluorescence, the scaled fluorescence excitation spectrum, $F^{*}_{PSII}(\lambda)$, $m^2(mg\ chl\ a)^{-1}$, is obtained. In contrast to $a^{*}_{\phi}(\lambda)$, the $F^{*}_{PSII}(\lambda)$ does not include the signatures from photoprotective carotenoids and PSI (Johnsen and Sakshaug 1993, Johnsen et al. 1997). By spectral weighting, the fraction of absorbed light received by LHCII and transferred to PSII can be calculated ($\overline{a}^{*}_{PSII}$, Fig. 1; Johnsen and Sakshaug 2007).

Usually, the PAM technique is used to determine photosynthetic variables on a relative scale, such as the quantum yield of charge separation (Φ_{PSII}) or the rate of PSII electron transport (rETR). These variables can be used to determine, on a relative scale, the production of algae in aquatic systems. Investigations into whether and how the variable fluorescence measurements can be related to photosynthetic oxygen production (P_{PSII}) have been attempted by Kolber and Falkowski (1993), Schreiber et al. (1995), Gilbert et al. (2000), Kromkamp et al. (2001), and Longstaff et al. (2002). However, to our knowledge, no attempt has been made to differentiate between absorption of light by PSII and PSI and their respective LHCs to obtain P_{PSII}. So far, it has been assumed that PSII and PSI absorb light in equal proportions irrespective of the species in question (Schreiber et al. 1986, Kolber and Falkowski 1993, Gilbert et al. 2000, Kromkamp and Forster 2003).

This study focuses on methods for determining photosynthetic oxygen-production rate based on in vivo variable fluorescence. We have tested three different approaches to estimate the fraction of light absorbed by PSII to find out if the PAM-based technique can be used in combination with biooptics to determine photosynthetic parameters in terms of oxygen production. The results are derived from experiments during which the oxygen evolution and the in vivo fluorescence measurements were conducted simultaneously in the PAM measurement cuvette.

MATERIALS AND METHODS

Algal cultures. Unialgal cultures originating from the culture collection of Trondhjem Biological Station—*Prorocentrum minimum*, *Prymnesium parvum* cf. *patelliferum*, and *Phaeodactylum tricornutum*—were grown in semicontinuous cultures in 5 L flasks with f/2 medium (Guillard and Ryther 1962), prefiltered (0.2 μm sterile filters pasteurized at 80°C in 3 h), and enriched with silicate (*P. tricornutum* only). They were then grown at 15 ± 1°C, salinity of 33, and constantly bubbled with filtered air. The illumination was continuous ''white'' fluorescent light

(Philips TLD 36W/96; Guilford, Surrey, UK) providing 80 $\mu mol \cdot m^{-2} \cdot s^{-1}$. The growth rate and the chl *a* concentration were maintained in a semiconstant state by diluting the cultures once per day, corresponding to a specific growth rate at 0.2 $\mu \cdot d^{-1}$ for *P. minimum* and *P. parvum*, and 0.7–0.8 $\mu \cdot d^{-1}$ for *P. tricornutum*, both prior to and during the experiments. The stock cultures were enriched with 1 g $NaHCO_3 \cdot L^{-1}$ to avoid depletion of inorganic carbon.

While growing, the physiological state of the cultures was monitored daily by measuring the ratio of in vivo chl *a* fluorescence before and after addition of DCMU [3(3,4 dichlorophenyl)-1,1-dimethylurea, 50 μM final concentration] in a Turner Designs fluorometer (Sunnyvale, CA, USA). A ratio of DCMU-fluorescence to fluorescence of >2.5 indicates a healthy state of the culture (Sakshaug and Holm-Hansen 1977). In our study, the ratio generally ranged from 2.7 to 3.5.

Experimental setup. PAM fluorescence measurements and oxygen-evolution rate were made simultaneously in a temperature-controlled plastic cuvette (Fig. 2). Prior to incubations, a subsample of 100 mL was placed in a temperature-controlled water bath at 10°C or 20°C for 30 min, keeping the irradiance constant. Subsequently, 2.7 mL of the sample was inserted into the cuvette, which was sealed with no headspace of air, using a lid housing a Peltier cell of constant temperature (±0.2°C, Walz, Effeltrich, Germany, US-T/S). The algae were kept suspended inside the cuvette by a slowly circulating water flow driven by the cooling of the Peltier cell and heating of the incubator light.

Subsamples were kept in the dark for 15 min prior to generating photosynthesis versus irradiance (*P* vs. *E*) curves. Both *P* versus *E* data for oxygen production and PAM fluorescence were measured during 10 min incubations followed by stepwise increase of the irradiance, from 1 to 500 μmol photons $\cdot m^{-2} \cdot s^{-1}$. The incubator light source was a slide projector equipped with a halogen lamp, and the light passed an IR filter (cutoff at 695 nm) in front of the PAM detector and slide frames with different layers of spectrally neutral mosquito netting.

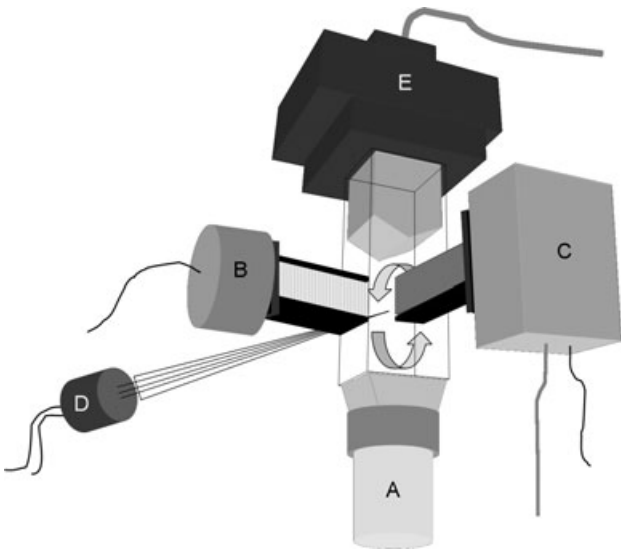

FIG. 2. A schematic drawing of the experimental setup. (A) Fiber optics to lead incubator light and flash light through a short pass filter (SP 695 nm) to the sample in the cuvette. (B) Probe light, a red light-emitting diode (LED, <0.15 μmol photons$\cdot m^{-2} \cdot s^{-1}$, 655 nm, 1.6 kHz and 100 kHz) with an excitation filter (SP 695 nm). (C) Photomultiplier detector (PMT, Walz, PM-101/N) with emission filter (LP 695 nm). (D) O_2-microsensor inserted through a tight-fitting miniature pipe in the wall of the incubation cuvette. (E) A Peltier cell in which the temperature was kept constant (±0.2°C, Walz, US-T/S). The algae were kept suspended inside the cuvette by a slowly circulating water flow driven by the cooling of the Peltier cell and heating from the incubator light.

Irradiance measurements. The growth irradiance was measured inside the culture flasks filled with sterile seawater, using a scalar (4π) irradiance sensor (QSL-100; Biospherical Instruments, San Diego, CA, USA). The incubation irradiance (PAR) was measured inside the (PAM cuvette) incubation chamber, using a cosine-corrected (2π) light collector on the DIVING-PAM (Walz). The spectral distribution of the incubation light was measured using a RAMSES spectroradiometer (TRIOS, Oldenburg, Germany) from 400 to 850 nm with 1 nm resolution. The irradiance and the spectral distribution of the incubation light were used for calculating light absorbed by PSII.

PAM measurements. Fluorescence was measured using a PAM-101 fluorometer with a 102 and 103 module (Walz; Schreiber et al. 1986) equipped with a photomultiplier detector (PMT, Walz, PM-101/N; Fig. 2). A red light-emitting diode (655 nm peak, <0.15 μmol photons$\cdot m^{-2} \cdot s^{-1}$, at 1.6 kHz) was used as probe light at an intensity too low to induce significant variable fluorescence. In the following we used the nomenclature of van Kooten and Snel (1990). The minimum fluorescence (F_o) and the maximum fluorescence (F_m) were measured at the end of the dark-acclimation period (15 min), when approximately all RCs were closed. F_m was measured during exposure to a saturating light pulse from a halogen lamp (0.6 s at >5,000 μmol photons$\cdot m^{-2} \cdot s^{-1}$; KL1500 electronic, Schott, Mainz, Germany), which illuminated the sample via an optical fiber. The F_o and F_m values obtained from the DA 100 software were not used. Instead an average of 150 data points from the initial fluorescence was used to determine F_o, and an average of 200 data points from the maximum fluorescence was used to determine F_m using an Excel worksheet (Microsoft Corp., Redmond, WA, USA). The maximum quantum yield of PSII charge separation (Φ_{PSII_max}) in the dark-acclimated cells was calculated as

$$\Phi_{PSII\_max} = F_v/F_m = \frac{F_m - F_0}{F_m} \quad (1)$$

Under actinic illumination, the operational quantum yield of PSII (Φ_{PSII}) was calculated from the steady-state fluorescence (F_0') and the maximum fluorescence after a saturation pulse (F_m') at each incubation irradiance (Genty et al. 1989):

$$\Phi_{PSII} = \Delta F/F_m' = \frac{F_m' - F_0'}{F_m'} \quad (2)$$

O_2 measurements. Net O_2-production rate was measured as the O_2 concentration change during incubation for each irradiance by a Clark-type O_2 microsensor (Revsbech 1989) inserted through a tight-fitting miniature pipe in the wall of the incubation cuvette (Fig. 2). The sensor had an external tip diameter of ~100 μm, stirring sensitivity of <1.5%, and a 90% response time of <4 s. Prior to the measurements, the electrode was calibrated by a two-point calibration both in anoxic and air-saturated seawater at the specific temperature (Glud et al. 2000). The sensor current was measured using a picoammeter (PA 2000; Unisense, Aahus, Denmark) connected to a strip-chart recorder (Kipp and Zonen, Delft, the Netherlands) and a PC. The dark-respiration rate was measured during the last 10 min of the dark period prior to the light incubations. The photosynthetic O_2-production rate (P_{O2}) was calculated by adding the dark-respiration rate to the net O_2-production rate.

Biooptical measurements. In order to calculate oxygen evolution per biomass and time on the basis of measurements of Φ_{PSII}, it is necessary to estimate the light absorbed by PSII in

absolute units. Such a calculation requires knowledge of the in vivo chl *a*–specific absorption coefficient [$a^*_\phi(\lambda)$] and the PSII-scaled in vivo fluorescence excitation spectrum [$F^*_{PSII}(\lambda)$; Johnsen et al. 1997]. We obtained $a^*_\phi(\lambda)$ and $F^*_{PSII}(\lambda)$ (Fig. 1) by measuring the optical density [$OD(\lambda)$] of phytoplankton cells collected on glass fiber filters (Whatman GF/F, Maidstone, UK) in a dual-beam spectrophotometer (Hitachi 150-20; Hitachi, San Jose, CA, USA), using a clean filter wetted with filtered seawater as reference (Yentsch 1962, Mitchell and Kiefer 1988). Three replicate spectra were measured from 350 to 800 nm at 1 nm increments, and the average OD from 750 to 800 nm was subtracted from the whole spectrum to correct for light scattering (Mitchell and Kiefer 1988). OD of the filter with algae (OD_{filt}) was converted into OD in suspension (OD_{susp}) using a second-order polynomial expression (β-correction, eq. 3, Mitchell 1990).

$$OD_{susp}(\lambda) = m_1 \cdot OD_{filt}(\lambda) + m_2 \cdot [OD_{filt}(\lambda)]^2 \quad (3)$$

The parameters m_1 and m_2 have been determined based on laboratory cultures: $m_1 = 0.508$ and $m_2 = 0.134$ for *P. parvum* (Chauton et al. 2004); and $m_1 = 0.221$ and $m_2 = 0.577$ for *P. minimum*; and for *P. tricornutum,* values for *Skeletonema costatum* were used ($m_1 = 0.407$ and $m_2 = 0.602$, R. Sandvik unpublished data) because of their similar pigmentation and size. Absorption (a, m^{-1}) was calculated from OD_{susp} according to equation 4:

$$a = 2.3 \cdot OD_{susp}(\lambda) \cdot (S/V) \quad (4)$$

where S is the clearance rate of GF/F filter (mm^2), and V is the volume (mL) of the filtered sample (Mitchell and Kiefer 1988).

The chl *a* concentration was measured on extracts from the filters that were used for in vivo light absorption, using a spectrophotometer (Hitachi 150-20). Immediately after the in vivo light absorption measurement, the filters were extracted in precooled 100% methanol (4°C, 5 mL) for 3 h in glass centrifuge tubes. The tubes were placed in the dark at 4°C and stirred for 10 s in a Vortex-mixer after 0, 1.5, and 3 h. The extracts were refiltered (0.2 μm polycarbonate filter) before measuring OD from 350 to 800 nm. The chl *a* concentration ($mg \cdot m^{-3}$) was calculated using the extinction coefficient for chl *a* in methanol at 665 nm, 74.5 $L \cdot g^{-1} \cdot cm^{-1}$ (MacKinney 1941).

The chl *a*–specific absorption coefficient [$a^*_\phi(\lambda)$, m^2 (mg chl *a*)$^{-1}$] was determined by normalizing the absorption spectrum (m^{-1}) to the chl *a* concentration ($mg \cdot m^{-3}$, Fig. 1).

In vivo fluorescence excitation spectra were measured using a spectrofluorometer (Hitachi F-3000). An infrared-transmitting glass filter (Schott RG 695 IR) was placed in front of the photomultiplier to prevent direct and scattered light from the light source and cells. Prior to the measurements, a time scan was recorded with DCMU-treated cells (50 μM final concentration) during 1.5 min (scan time for a full spectrum) avoiding nonvariable chl *a* fluorescence signal (Johnsen and Sakshaug 1993). The in vivo chl *a* fluorescence excitation spectra were recorded with excitation wavelengths from 400 to 700 nm (5 nm bandwidth), and emission was monitored at 730 nm (5 nm bandwidth, Neori et al. 1988). The data were recorded at 1 nm resolution. All fluorescence excitation measurements were quantum corrected using the dye Basic Blue 3 (Kopf and Heinze 1984, Sakshaug et al. 1991).

Scaling of the fluorescence excitation spectra followed the no-overshoot procedure (Johnsen et al. 1997, Johnsen and Sakshaug 2007) by matching the fluorescence spectra to the corresponding absorption spectra at selected wavelengths, yielding a PSII-scaled fluorescence excitation spectrum, $F^*_{PSII}(\lambda)$. The matchpoint preventing overshoot was ~550 nm for *P. minimum* and *P. parvum*, except that for *P. minimum* at 20°C, it was ~650 nm (Fig. 3). *P. tricornutum* exhibited matchpoints in the red band, 675–685 nm (Fig. 3). The no-overshoot procedure yields an upper limit for the number of quanta absorbed by PSII (Johnsen and Sakshaug 2007).

Particulate organic carbon (POC). POC was measured on filtered subsamples (Whatman GF/F, baked) and analyzed after treatment of the samples with fuming hydrochloric acid (Carlo Erba Elemental Analyzer Model Na; Carlo Erba, Milan, Italy).

Calculation of the oxygen production rate, P_{PSII}. Oxygen production rate (P_{PSII}) can be calculated as follows:

$$P_{PSII} = \Phi_{PSII} \cdot E \cdot \Gamma \cdot AQ_{PSII} \quad (5)$$

Φ_{PSII} is the quantum yield of charge separations in PSII (mol $e^- \cdot$ mol photon^{-1}, Genty et al. 1989), and E is the irradiance (μmol photons $\cdot m^{-2} \cdot s^{-1}$), which multiplied by Φ_{PSII} yields the relative electron transfer rate (rETR). Γ is the stoichiometric ratio of oxygen evolved per electron generated at PSII. According to the standard Z-scheme of photosynthesis, four stable charge separations are needed in each PSI and PSII to release one O_2 molecule. Γ, accordingly, is 0.25 $O_2 \cdot (e^-)^{-1}$ (Kroon et al. 1993, Gilbert et al. 2000). Empirically, a quantum requirement (QR) higher than eight photons has been observed, caused by different sinks for photosynthetic electron transport, for example, Mehler-type reactions and photorespiration (Kromkamp et al. 2001, Longstaff et al. 2002). For simplicity, we assumed Γ = 0.25. AQ_{PSII} represents quanta absorbed by PSII [m^2(mg chl *a*)$^{-1}$].

With the aim to quantify the O_2-production rate from PAM fluorescence in absolute units, we tested three different approaches for estimating AQ_{PSII}.

1) $AQ_{PSII} = 0.5 \cdot \overline{a}^*_\phi$. The commonly used correction factor 0.5 implies that absorbed light is equally distributed among PSI and PSII (Schreiber et al. 1986, Kolber and Falkowski 1993, Kroon et al. 1993, Gilbert et al. 2000, Morris and Kromkamp 2003).

2) $AQ_{PSII} = F_{II} \cdot \overline{a}^*_\phi$. F_{II} is the fraction of chl *a* in PSII determined from the ratio between the scaled (no-overshoot) red-peak fluorescence excitation and the red absorption peak [$a^*_{PSII}(red)/a^*_\phi(red)$] (Johnsen et al. 1997; Figs. 1 and 3).

3) $AQ_{PSII} = \overline{a}^*_{PSII}$. This factor represents light absorbed by PSII, determined from the scaling of the fluorescence excitation to the absorption spectra by the no-overshoot procedure (Johnsen et al. 1997; Figs. 1 and 3).

Both $a^*_\phi(\lambda)$ and $F^*_{PSII}(\lambda)$ were spectrally weighted from 400 to 700 nm (eq. 6):

$$\overline{X} = \frac{\left[\sum_{400}^{700} X(\lambda)E(\lambda)d\lambda\right]}{E(PAR)} \quad (6)$$

$\overline{X}$ is the spectrally weighted chl *a*–specific absorption coefficient ($\overline{a}^*_\phi$) or the spectrally weighted PSII absorption ($\overline{a}^*_{PSII}$), X is $a^*_\phi(\lambda)$ or $F^*_{PSII}(\lambda)$, and $E(\lambda)$ is the incubation irradiance.

Curve fitting. The P versus E curves were fitted to data using a nonlinear least-squares procedure (SigmaPlot 9.0, SYSTAT Sotfware Inc., San Jose, CA, USA) using the equation by Webb et al. (1974, eq. 7). The photosynthetic parameters, the maximum photosynthetic rate (P_{max}), and the maximum light utilization coefficient (α) were calculated for each curve. The light saturation parameter (E_k) was calculated as P_{max}/α. Notation of the photosynthetic parameters (Table 1) follows Sakshaug et al. (1997).

$$P = P_{max}\left[1 - \exp\left(\frac{-\alpha \cdot E}{P_{max}}\right)\right] \quad (7)$$

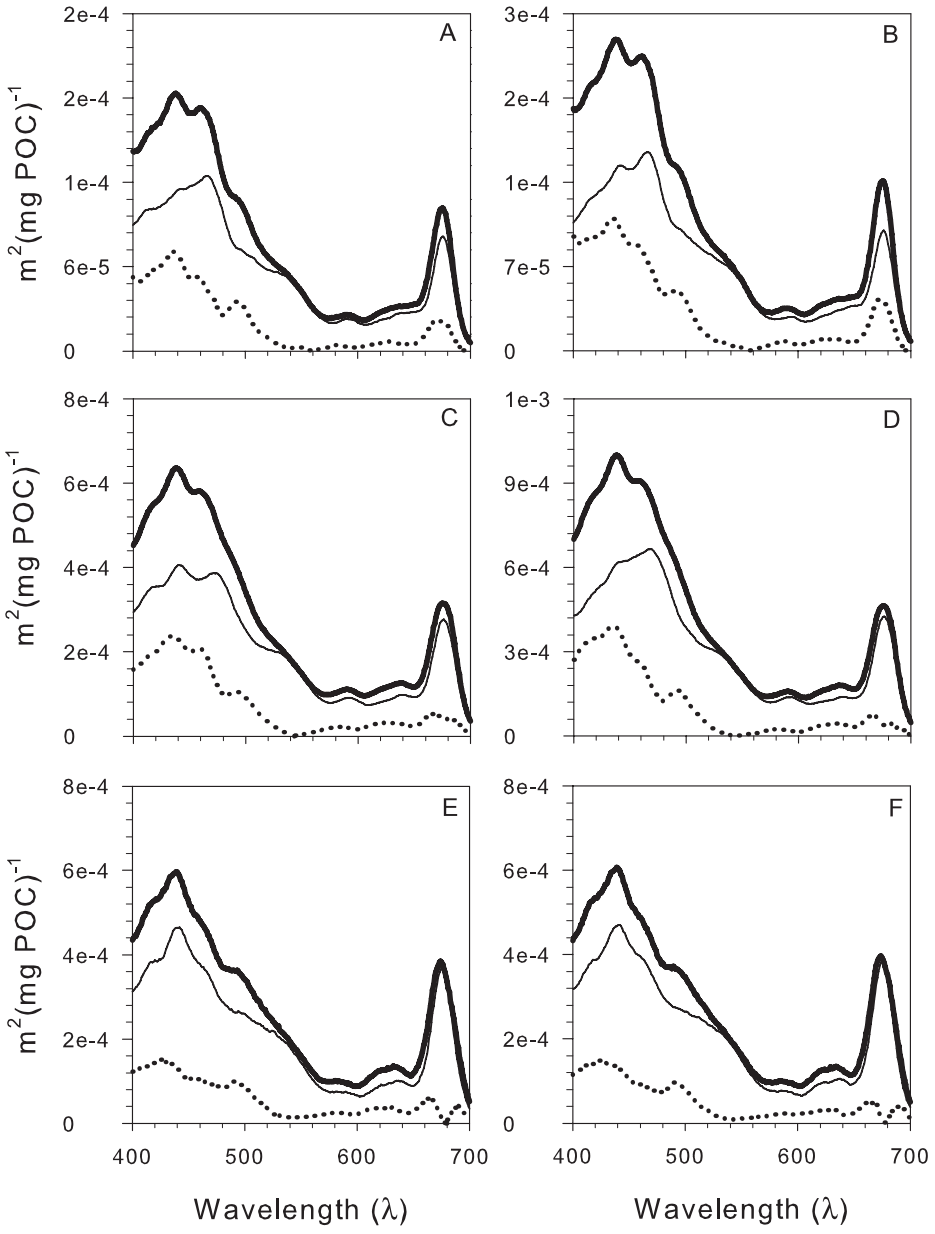

FIG. 3. In vivo POC-specific absorption coefficients, $a^*_\phi(\lambda)$ (thick black line), the PSII-scaled fluorescence excitation spectra, $F^*_{PSII}(\lambda)$ (thin black line) and the corresponding difference spectra, $[a^*_\phi(\lambda) - F^*_{PSII}(\lambda)$, dotted black line] for *Prorocentrum minimum* (A, B), *Prymnesium parvum* (C, D), and *Phaeodactylum tricornutum* (E, F), at 10°C (left column) and 20°C (right column). The difference spectra denote the nonfluorescent fraction indicating absorption of PSI and photoprotective pigments (diadinoxanthin and diatoxanthin). POC, particulate organic carbon.

RESULTS

The total amount of absorbed light ($\overline{a}^*_\phi$) ranged from 0.0068 to 0.0164 m^2(mg chl *a*)$^{-1}$, *P. parvum* exhibiting the highest, and *P. minimum*, the lowest absorption coefficients (Table 2).

The fraction of chl *a* in PSII (F_{II}) ranged from 70% to 98% (Table 2). For *P. tricornutum*, F_{II} was 97% and 98% for the 10°C and 20°C incubations, respectively. *P. minimum* exhibited the lowest coefficients, 80% and 70% for 10°C and 20°C, respectively. The fraction of light absorbed by PSII ($\overline{a}^*_{PSII}$) ranged from 0.0054 to 0.0132 m^2(mg chl *a*)$^{-1}$, with *P. parvum* and *P. minimum* exhibiting the highest and lowest fractions, respectively (Table 2).

The coefficient of variance (CV, %) for the estimation of F_o and F_m (after 15 min of preincubation in darkness) was generally small. At maximum irradiance (494 μmol photons·m^{-2}·s^{-1}), the CVs for F_o' and F_m' were generally larger than in darkness. The F_o value for *P. parvum* (10°C) was 0.246 ± 2%, and the F_o' value was 0.166 ± 22%. The F_m value was 0.881 ± 2%, and the F_m' value was 0.175 ± 4%. For *P. minimum* (10°C), the F_o and F_o' were 0.223 ± 27% and 0.142 ± 47%, respectively. The F_m value was 0.564 ± 3%, and the F_m' value was 0.155 ± 10%. The F_o and the F_o' values for *P. tricornutum* (10°C) were 0.152 ± 11% and 0.116 ± 8%, respectively. The F_m value was 0.465 ± 4%, and the F_m' value was 0.122 ± 8%.

TABLE 1. Significant symbols.

Symbol	Explanation	Dimension
$a^*_\phi(\lambda)$	Chl *a*–specific absorption coefficient, 400–700 nm	$m^2(mg\ chl\ a)^{-1}$
$F^*_{PSII}(\lambda)$	PSII-scaled fluorescence excitation spectrum, 400–700 nm	$m^2(mg\ chl\ a)^{-1}$
$\overline{a}^*_\phi$	Total amount of spectrally weighted light absorbed normalized to chl *a*	$m^2(mg\ chl\ a)^{-1}$
$\overline{a}^*_{PSII}$	Spectrally weighted PSII-absorption normalized to chl *a*	$m^2(mg\ chl\ a)^{-1}$
F_{II}	Fraction of chl *a* in PSII and its associated LHC, $[F^*_{PSII}(red)/a^*_\phi(red)]$	
P_{PSII}	Calculated O_2-production rate at a given *E*	$mg\ O_2(mg\ POC)^{-1}\cdot h^{-1}$
P_{PSII_max}	Calculated O_2-production rate at light saturation	$mg\ O_2(mg\ POC)^{-1}\cdot h^{-1}$
P_{O2}	Oxygen-production rate at a given irradiance	$mg\ O_2(mg\ POC)^{-1}\cdot h^{-1}$
P_{O2_max}	Maximum oxygen-production rate at light saturation	$mg\ O_2(mg\ POC)^{-1}\cdot h^{-1}$
α	Maximum light utilization coefficient	$mg\ O_2(mg\ POC)^{-1}\cdot h^{-1}\ (\mu mol\ photons\cdot m^{-2}\cdot s^{-1})^{-1}$
E_k	Light saturation parameter (P_{max}/α)	$\mu mol\ photons\cdot m^{-2}\cdot s^{-1}$
Γ	Stoichiometric ratio of oxygen evolved per electron generated at PSII	$O_2\cdot(e^-)^{-1}$
F_0	Initial fluorescence in dark-acclimated cells	
F_0'	Initial fluorescence in cells incubated in actinic light	
F_m	Maximum fluorescence in dark-acclimated cells	
F_m'	Maximum fluorescence in cells incubated in actinic light	
F_v	Variable fluorescence in dark-acclimated cells	
F_v'	Variable fluorescence in cells incubated in actinic light	
Φ_{PSII_max}	Maximum quantum yield of charge separation in PSII	$mol\ e^-\cdot mol\ photons^{-1}$
Φ_{PSII}	Operational quantum yield of charge separation in PSII	$mol\ e^-\cdot mol\ photons^{-1}$
${}^{PSII}\Phi_{O2\_max}$	Maximum quantum yield of O_2-production rate, using $\overline{a}^*_{PSII}$	$mol\ e^-\cdot mol\ photons^{-1}$

TABLE 2. Chl *a* concentration ($\mu g\cdot L^{-1}$), carbon content (POC, $\mu g\cdot L^{-1}$), and chl $a\cdot C^{-1}$ ratio (w:w) in the cultures during each experiment. Fraction of chl *a* in PSII calculated from red-peak scaling (F_{II}), spectrally weighted PSII absorption normalized to chl *a* ($\overline{a}^*_{PSII}$; $m^2\ [mg\ chl\ a]^{-1}$ or $[mg\ chl\ a]^{-1}\cdot h^{-1}$), and the spectrally weighted light absorption coefficient normalized to chl *a* ($\overline{a}^*_\phi$; $m^2\ [mg\ chl\ a]^{-1}$) for each incubation.

Species	Incubation temperature (°C)	[chl *a*]	POC	chl $a\cdot C^{-1}$	F_{II}	$\overline{a}^*_{PSII}$	$\overline{a}^*_\phi$
Prorocentrum minimum	10	312.3	37,396	0.0084	0.801	0.0054	0.0068
	20	281.0	29,060	0.0097	0.702	0.0062	0.0082
Prymnesium parvum	10	711.4	36,887	0.0193	0.873	0.0084	0.0108
	20	689.0	36,319	0.0190	0.922	0.0132	0.0164
Phaeodactylum tricornutum	10	135.0	6,323	0.0213	0.966	0.0076	0.0095
	20	205.8	8,319	0.0247	0.975	0.0068	0.0083

POC, particulate organic carbon.

P versus *E* curves for the O_2-production rate, measured with O_2 microsensors (P_{O2}) and calculated from the operational quantum yield of PSII (Φ_{PSII}) in combination with the three biooptical approaches (P_{PSII}), showed the typical *P* versus *E* shape with a nearly linear initial slope (α) and increasing saturation (P_{max}) with increasing irradiance. None of the curves showed a decrease in *P* at high irradiances; thus, photoinhibition was not observed.

PAM-derived photosynthetic parameters were compared to parameters derived from direct O_2 measurements (Fig. 4). The photosynthetic parameters derived from PAM measurements are gross O_2 production, since it measures the rETR rate in PSII and is not influenced by O_2 respiration. From the O_2-microsensor technique, net O_2 production was measured. By adding the O_2 respiration in the dark, gross O_2 production was estimated. However, this underestimates the gross O_2 production due to an enhanced O_2 respiration under illumination compared to the dark respiration (Ludden et al. 1985, Glud et al. 1992, Canfield and DesMarais 1993). Consequently, rates of P_{PSII} (based on PAM fluorescence) should theoretically be higher than P_{O2} rates (measured by O_2 microsensors).

The maximum production rate for P_{O2} (P_{O2_max}) was ~2 times higher (1.5–2.4) in cultures incubated at 20°C than at 10°C (Fig. 4, Table 3), as expected according to a Q_{10} of ~2 normally observed for phytoplankton (Davison 1991, Hancke et al. 2008).

For P_{PSII}, the maximum O_2-production rate (P_{PSII_max}) was normally highest when based on $F_{II}\cdot\overline{a}^*_\phi$ (approach 2), followed by $\overline{a}^*_{PSII}$ (approach 3), and was lowest when based on $0.5\cdot\overline{a}^*_\phi$ (approach 1, Fig. 4, Table 3). Overall, P_{PSII} exhibited the same trend as P_{O2}, except for *P. minimum* at 20°C, which yielded P_{PSII_max} ~2 times lower than P_{O2_max}, and for *P. parvum* at 20°C where P_{PSII_max} values were ~2 times higher. For the other incubations, the range of values for P_{PSII_max} was in the same area as the value of P_{O2_max} (Fig. 4, Table 3).

The light saturation parameter (E_k) showed a pattern opposite of that for P_{max}, implying that E_k was higher when calculated on the basis of P_{PSII} than

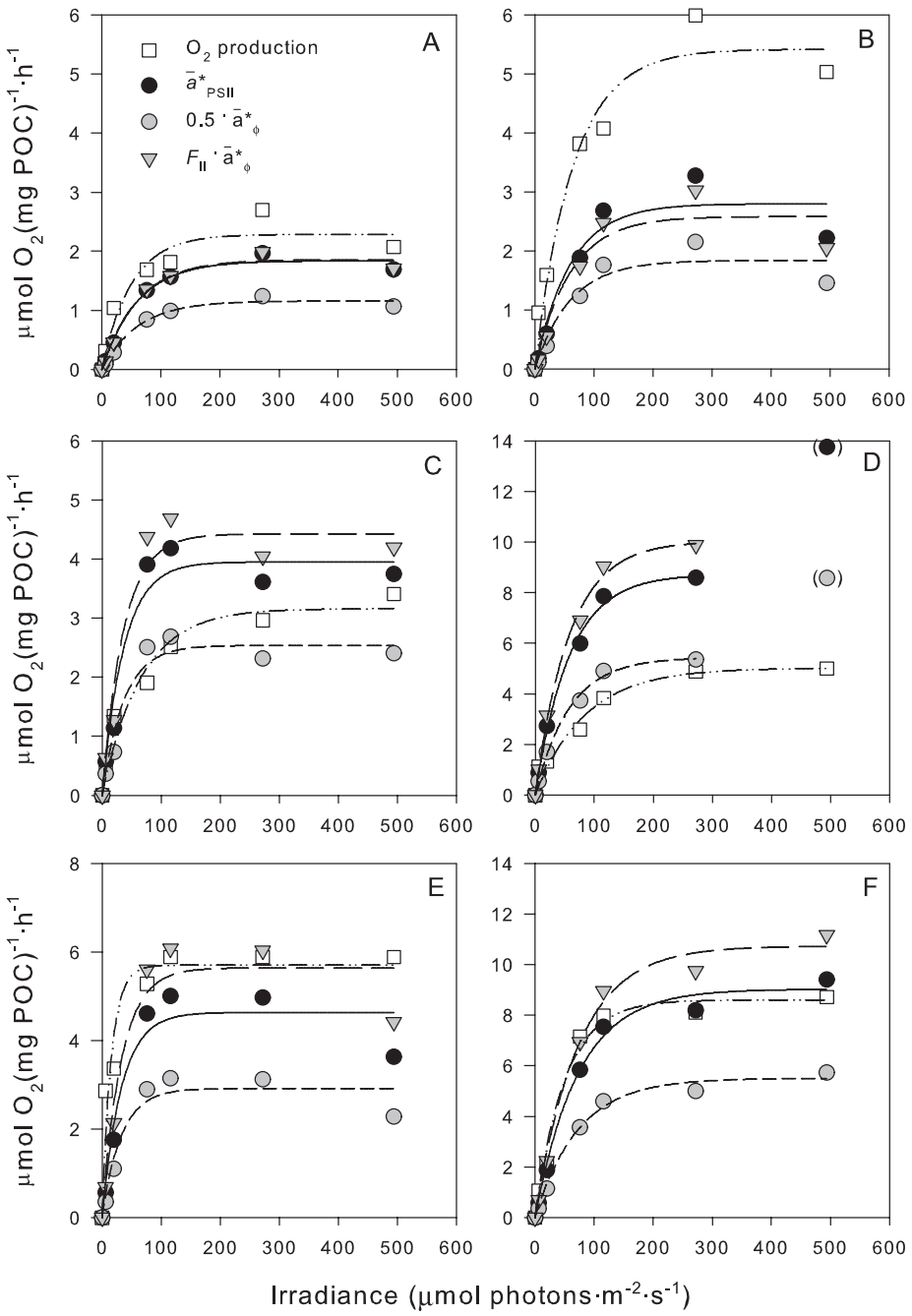

FIG. 4. Photosynthesis versus irradiance curves calculated from PAM fluorescence measurements (P_{PSII}) based on three biooptical approaches for estimation of light absorbed by PSII, AQ_{PSII}: $0.5 \cdot \overline{a}^*_\phi$ (approach 1), $F_{II} \cdot \overline{a}^*_\phi$ (approach 2), and $\overline{a}^*_{PSII}$ (approach 3) and simultaneously measured photosynthetic O_2 evolution (P_{O2}) for *Prorocentrum minimum* (A, B), *Prymnesium parvum* (C, D), and *Phaeodactylum tricornutum* (E, F), at 10°C (left column) and 20°C (right column). Parentheses in (D) denote outliers. Note different *y*-axes. PAM, pulse amplitude modulated.

P_{O2} for *P. minimum* and *P. tricornutum*, and lower for *P. parvum* (Fig. 4, Table 3).

To find the best linear fit between calculated and measured maximum oxygen production, P_{PSII_max}, estimates based on three biooptical approaches were plotted as a function of P_{O2_max} (Fig. 5a). Approaches 1, 2, and 3 gave slope coefficients of 0.6 ($R^2 = 0.50$), 1.2 ($R^2 = 0.51$), and 1.0 ($R^2 = 0.51$), respectively. Approach 3 ($\overline{a}^*_{PSII}$) resulted in the slope coefficient closest to unity, implying that $\overline{a}^*_{PSII}$ provides the best fit for P_{PSII_max} to P_{O2_max}.

The relationship between the maximum light utilization coefficient (α) for P_{O2} and calculated values of α was tested by plotting α for P_{O2} against α for P_{PSII}, again using the three biooptical approaches (Fig. 5b). The linear regressions exhibited slopes of 0.12 ($R^2 = 0.22$), 0.26 ($R^2 = 0.27$), and 0.19 ($R^2 = 0.23$) for the three approaches, respectively (Fig. 5b), indicating a weak relationship.

We analyzed the relationship between P_{O2} and P_{PSII}, using $\overline{a}^*_{PSII}$, for the entire irradiance range for the three species investigated (Fig. 6). The relationship between P_{O2} and P_{PSII} was adequately described by a linear regression ($R^2 = 0.7$–0.97). The slope differed between the species, and in two cases, with the incubation temperature. *P. minimum*

TABLE 3. Photosynthetic parameters calculated from the P versus E curves in Figure 4 for P_{PSII}, using $\overline{a}^*_{PSII}$, $F_{II}\cdot\overline{a}^*_{\phi}$ and $0.5\cdot\overline{a}^*_{\phi}$, and P_{O2}.

		P_{PSII}							P_{O2}		
		P_{max}			α			E_k	P_{max}	α	E_k
Species	Incubation temperature (°C)	$\overline{a}^*_{PSII}$	$F_{II}\cdot\overline{a}^*_{\phi}$	$0.5\cdot\overline{a}^*_{\phi}$	$\overline{a}^*_{PSII}$	$F_{II}\cdot\overline{a}^*_{\phi}$	$0.5\cdot\overline{a}^*_{\phi}$	-	O_2-meas.	O_2-meas.	O_2-meas.
Prorocentrum minimum	10	1.839	1.857	1.158	0.030	0.030	0.019	61.0	2.285	0.046	49.8
	20	2.802	2.585	1.843	0.047	0.043	0.031	59.8	5.418	0.084	64.2
Prymnesium parvum	10	3.953	4.426	2.538	0.108	0.121	0.069	36.6	3.161	0.048	66.0
	20	8.728	10.040	5.440	0.150	0.173	0.094	58.1	5.020	0.059	84.7
Phaeodactylum tricornutum	10	4.636	5.638	2.915	0.142	0.171	0.089	32.8	5.698	0.362	15.7
	20	9.025	10.725	5.502	0.123	0.146	0.075	73.3	8.597	0.171	50.3

POC, particulate organic carbon.

incubated at 10°C exhibited a slope of 0.86 (R^2 = 0.94), and at 20°C, 0.59 (R^2 = 0.92) (Fig. 6a). This result indicates that P_{O2} is closely related to P_{PSII} estimates derived on the basis of the $\overline{a}^*_{PSII}$, and, moreover, that the two are linearly related. The slopes for *P. parvum* were 1.23 (R^2 = 0.70) and 2.5 (R^2 = 0.87) for 10°C and 20°C, respectively, suggesting that P_{PSII} overestimates P_{O2} by a factor of 1.2 at 10°C and 2.5 at 20°C (Fig. 6b). The slopes for P_{O2} against P_{PSII} of *P. tricornutum* were 1.3 at 10°C (R^2 = 0.89) and 1.0 at 20°C (R^2 = 0.97), not significantly different from unity (Fig. 6c). Consequently, the relationship between P_{O2} and P_{PSII} did not differ between the two incubation temperatures, predicting a linear relationship near unity for the entire P verus E curve.

DISCUSSION

We have tested three biooptical approaches to determine the fraction of light absorbed by PSII. In combination with PAM fluorescence, they were subsequently evaluated against measured rates of oxygen production. This approach made it possible to improve the quality of estimates for the O_2-production rate in absolute units from PAM-based fluorescence. Johnsen and Sakshaug (2007) suggested that $\overline{a}^*_{PSII}$ is the most accurate and direct measure of light absorbed by PSII, whereas F_{II} only corrects for light absorbed by PSII and not the photoprotective carotenoids. F_{II}, therefore, overestimates the light absorbed by PSII and, consequently, the O_2-production rate. In addition, presupposing that light is equally absorbed by PSII and PSI underestimates the absorption by PSII and the O_2-production rate in chromophytes by ~20%.

The fraction of chl *a* in PSII calculated from of F_{II} (Table 2) was high compared to approach 1. High compared to those suggested by Johnsen and Sakshaug (2007), our F_{II} values might be associated with our high OD_{filt} readings in the 550–600 nm bands, where OD otherwise is typically low. In the same context, uncoupling of LHC from PSII will enhance state II-I transitions (Mullineuax and Allen 1988, Kroon et al. 1993), which may cause high F_{II} values.

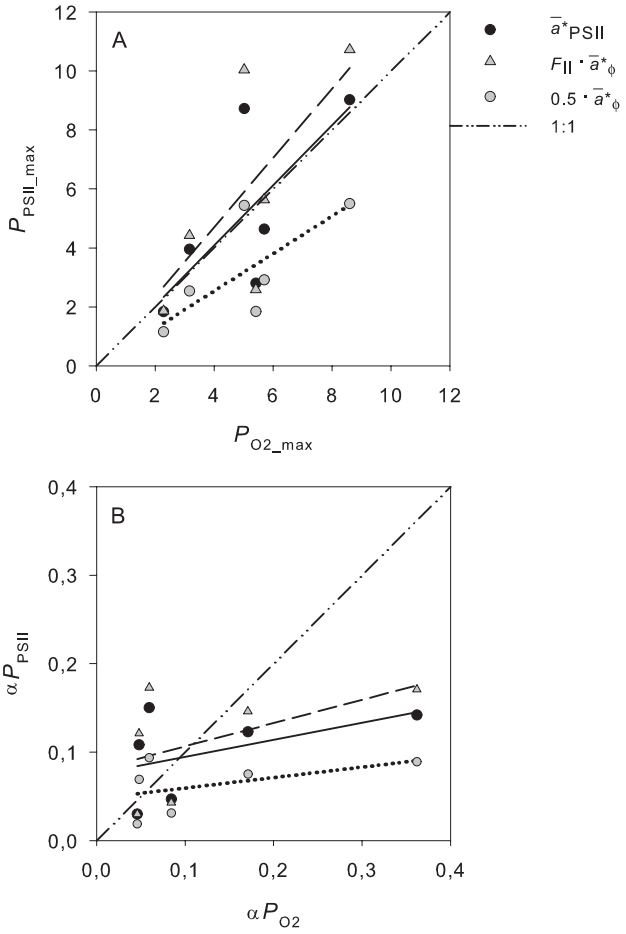

FIG. 5. (A) Maximum photosynthetic rate, P_{PSII_max}, based on $\overline{a}^*_{PSII}$, $F_{II}\cdot\overline{a}^*_{\phi}$, and $0.5\cdot\overline{a}^*_{\phi}$, as function of P_{O2_max}, for the six incubations (three species: *Prorocentrum minimum*, *Prymnesium parvum*, and *Phaeodactylum tricornutum*; and two temperatures: 10°C and 20°C). Units on both axes are μmol O_2(mg POC)$^{-1}\cdot h^{-1}$. (B) αP_{PSII} calculated from $\overline{a}^*_{PSII}$, $F_{II}\cdot\overline{a}^*_{\phi}$, and $0.5\cdot\overline{a}^*_{\phi}$, as function of αP_{O2}, for the same six incubations. Units on both axes are μmol O_2(mg POC)$^{-1}\cdot h^{-1}$ (μmol photons$\cdot m^{-2}\cdot s^{-1})^{-1}$. The dashed line represents $x = y$.

Representing total absorbed by PSII, $F_{II}\cdot\overline{a}^*_{\phi}$ can yield values too high for P_{PSII}. On the other hand, $0.5\cdot\overline{a}^*_{\phi}$ usually underestimates P_{O2} because the PSII:PSI ratio is higher for nearly all chromophyte

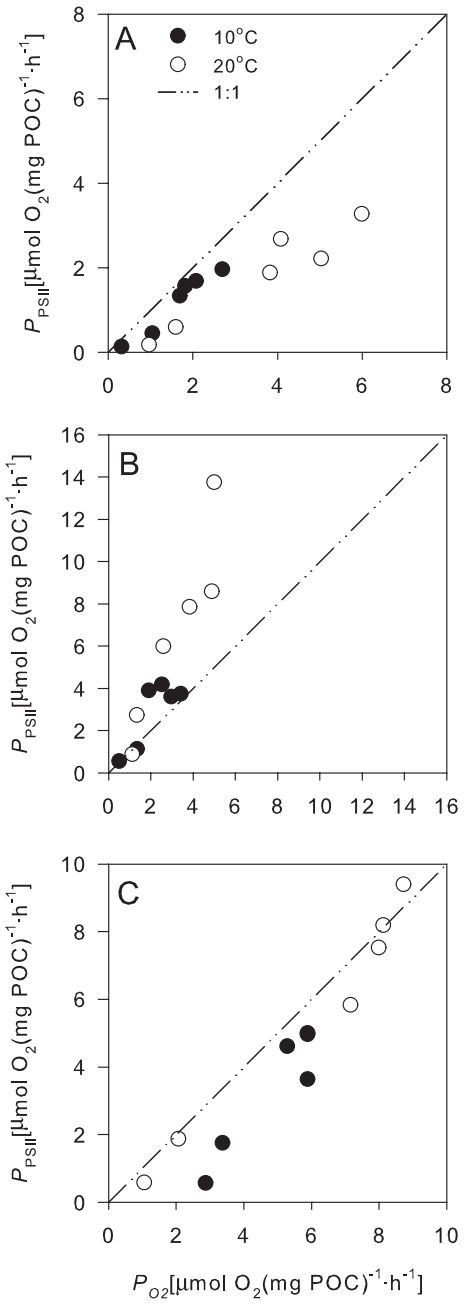

FIG. 6. P_{PSII} based on $\overline{a}^*_{PSII}$ as function of P_{O2} incubated at 10°C and 20°C, for (A) *Prorocentrum minimum*, (B) *Prymnesium parvum*, and (C) *Phaeodactylum tricornutum*. The dashed line represents $x = y$.

phytoplankton; Johnsen and Sakshaug (2007) suggest an average F_{II} of 0.72 for this group. In principle, $\overline{a}^*_{PSII}$ yields the most accurate estimate for light absorbed by PSII because it corrects for absorption by photoprotective carotenoids and PSI (Johnsen et al. 1997) and is therefore most suitable for calculating P_{PSII} on the basis of PAM data.

The PAM and the O_2-microsensor techniques have their limitations and strengths in terms of sensitivity and noise. In weak light ($E < E_k$), Φ_{PSII} is relatively high compared to E, yielding a robust measure of the rETR; thus, the estimation of α based on the PAM technique is reliable. Conversely, the microsensor technique is working near the detection limit in weak light and with a low signal-to-noise ratio, thus yielding low accuracy for α.

During light-saturated photosynthesis ($E > E_k$), the accuracy of the results from PAM and O_2-microsensor techniques, respectively, are opposite that for estimates of α. P_{max} based on PAM generates a small Φ_{PSII}:E ratio because Φ_{PSII} decreases with increasing E, causing low accuracy of rETR at high irradiance. In contrast, the signal-to-noise ratio of the O_2 microsensor increases with increasing irradiance, turning the method more reliable in the light-saturated part of the P versus E curve.

The operational quantum yield of oxygen production (Φ_{O2}) can be calculated (Flameling and Kromkamp 1998):

$$\Phi_{O_2} = \frac{P_{O_2}}{115 \cdot \mathrm{E} \cdot \overline{a}^*_{PSII}} \tag{8}$$

where 115 is a correction factor providing uniform dimensions, and P_{O2} is the chl *a*–specific oxygen production at each irradiance. Comparing Φ_{PSII} from PAM measurements and Φ_{O2} from O_2 measurements shows a positive correlation at high irradiance independent of species or temperature (Fig. 7). The exception is from data at low light measured with O_2 electrodes. As described, the signal-to-noise ratio at weak light is low, yielding uncertain data. The 4:1 line in Figure 7 indicates the relationship between Φ_{PSII} and Φ_{O2}, which illustrates the assumption of four photons in PSII yielding one oxygen molecule; thus, $\Gamma = 0.25$. For *P. minimum,* however, the ratio <4:1 indicates a quantum requirement (QR) lower than 4 to produce one oxygen molecule. In contrast, *P. parvum* exhibited QR >4:1. The Φ_{PSII}:Φ_{O2} ratio for *P. tricornutum* fits the 4:1 relationship well. Both Kromkamp et al. (2001) and Longstaff et al. (2002) observed QR values different from 4. The difference in QR in our material might cause the divergence between P_{O2} and P_{PSII} for *P. minimum* and *P. parvum* (P vs. E curves in Figs. 4 and 6).

Because our data in principle were collected simultaneously in the same experimental setup, they can be used to calculate the maximum quantum yield, ${}^{PSII}\Phi_{O2\_max}$ (Hancke et al. 2008) from the initial slope of the P versus E curve based on the O_2 measurements (α) and the fraction of light absorbed by PSII ($\overline{a}^*_{PSII}$):

$${}^{PSII}\Phi_{O2\_max} = \frac{\alpha^* P_{O2}}{\overline{a}^*_{PSII} \cdot 115} \tag{9}$$

where 115 is a correction factor ensuring uniform dimensions. On the basis of ${}^{PSII}\Phi_{O2\_max}$, we can in turn calculate the minimum quantum requirement (QR), which is the inverse of ${}^{PSII}\Phi_{O2\_max}$:

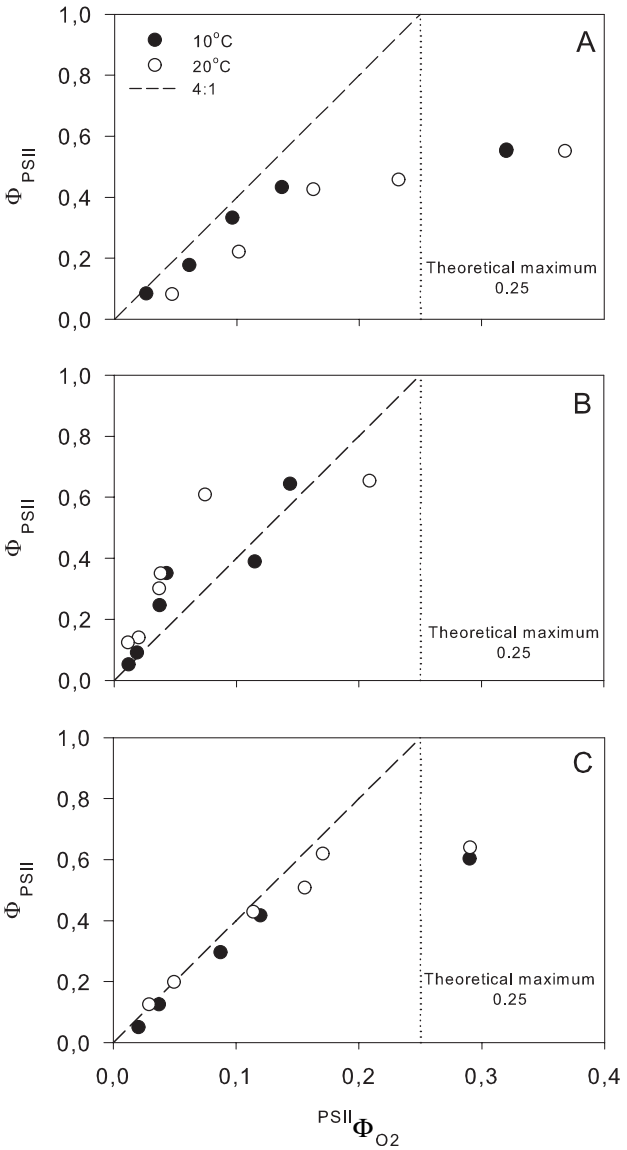

FIG. 7. Φ_{PSII} as a function of ${}^{PSII}\Phi_{O2}$ incubated at 10°C and 20°C, for (A) *Prorocentrum minimum*, (B) *Prymnesium parvum*, and (C) *Phaeodactylum tricornutum*. The dashed line represents the theoretical 4:1 relationship between Φ_{PSII} and ${}^{PSII}\Phi_{O2}$, indicating that four photons are needed to produce one oxygen molecule, yielding a maximum quantum yield of oxygen at 0.25; thus, $\Gamma = 0.25$.

$$QR = \frac{1}{{}^{PSII}\Phi_{O2\_max}} \quad (10)$$

Because of the questionable reliability of ${}^{PSII}\Phi_{O2\_max}$ and QR, they are not used in the calculations of P_{PSII}.

From our tests, $\overline{a}^*_{PSII}$ (approach 3) seems to provide the best input variable for calculating the oxygen-production rate from PAM measurements. This finding implies that $\overline{a}^*_{PSII}$ is the most relevant for light absorbed by PSII. The other two approaches overestimate ($F_{II} \cdot \overline{a}^*_{\phi}$, approach 2) or underestimate ($0.5 \cdot \overline{a}^*_{\phi}$, approach 1) the measured oxygen production, respectively.

Our results support the theory-based conclusions of Johnsen and Sakshaug (2007). Hence, we recommend $\overline{a}^*_{PSII}$ to estimate gross oxygen production from PAM fluorescence measurements.

The functional absorption cross-section of PSII RCs, σ_{PSII}, determined using fast-repetition-rate fluorometry is different from $\overline{a}^*_{PSII}$ because σ_{PSII} is determined from a narrow waveband (~20 nm centered around 478 nm) and has to be extrapolated to cover the 400–700 nm range (Falkowski and Chen 2003, Johnsen and Sakshaug 2007). It is not known to what extent σ_{PSII} is dependent on taxonomic and photophysiological differences in or between different pigment groups of phytoplankton (Suggett et al. 2004). Johnsen and Sakshaug (2007) examined 13 different pigment groups of phytoplankton, and they suggest that the known $\overline{a}^*_{PSII}$ can be used to correct for taxonomic and photoacclimative differences using all kinds of fluorometers.

In conclusion, variable fluorescence measurements in combination with biooptical measurements of light absorbed by PSII or values found in the literature (e.g., Johnsen and Sakshaug 2007) allow a noninvasive and fast determination of gross oxygen-production rate in phytoplankton. This technique might ease the work of primary-production measurements both in field and laboratory studies and might improve the accuracy of primary-production models in the future.

We thank the European Union financed programme SISCAL (IST 2000-28187), the Norwegian research council-financed Strategic University Programme MODTEQ (NFR # 128726/420), and the NORDKLIMA programme CABANERA (NFR # 155936/700) for financial support. In addition, we thank the Strategic University Program BIOROV (NTNU # 81111400) for a PhD research fellowship to T. B. H.

Canfield, D. E. & DesMarais, D. J. 1993. Biochemical cycles of carbon, sulphur, and free oxygen in microbial mat. *Geochim. Cosmochim. Acta* 57:3971–84.

Chauton, M. S., Tilstone, G. H., Legrand, C. & Johnsen, G. 2004. Changes in pigmentation, bio-optical characteristics and photophysiology, during phytoflagellate succession in mesocosms. *Photosynth. Res.* 26:315–24.

Davison, I. R. 1991. Environmental effects on algal photosynthesis – temperature. *J. Phycol.* 27:2–8.

Falkowski, P. G. & Chen, Y.-B. 2003. Photoacclimation of light harvesting systems in eukaryotic algae. *In* Green, B. R. & Parson, W.W. [Eds.] *Light-Harvesting Antennas in Photosynthesis.* Kluwer Academic Publishers, Dordrecht, the Netherlands, pp. 423–47.

Falkowski, P. G. & Woodhead, A. D. 1992. *Primary Productivity and Biochemical Cycles in the Sea.* Plenum Press, New York, 550 pp.

Flameling, I. A. & Kromkamp, J. 1998. Light dependence of quantum yields for PSII charge separation and oxygen evolution in eucaryotic algae. *Limnol. Oceanogr.* 43:284–97.

Genty, B., Briantais, J. M. & Baker, N. R. 1989. The relationship between the quantum yield of photosynthetic electron-transport and quenching of chlorophyll fluorescence. *Biochim. Biophys. Acta* 990:87–92.

Gilbert, M., Domin, A., Becker, A. & Wilhelm, C. 2000. Estimation of primary productivity by chlorophyll a in vivo fluorescence in freshwater phytoplankton. *Photosynthetica* 38:111–26.

Glud, R. N., Gundersen, J. K. & Ramsing, N. B. 2000. Electrochemical and optical oxygen microsensors for in situ measurements. *In* Buffle, J. & Horvai, G. [Eds.] *In Situ Monitoring of Aquatic Systems: Chemical Analysis and Speciation.* John Wiley & Sons, Chichester, UK, pp. 20–73.

Glud, R. N., Ramsing, N. B. & Revsbech, N. P. 1992. Photosynthesis and photosynthesis coupled respiration in natural biofilms quantified with oxygen microelectrodes. *J. Phycol.* 28:51–60.

Govindjee. 1995. Sixty-three years since Kautsky: chlorophyll *a* fluorescence. *Aust. J. Plant Physiol.* 22:131–60.

Guillard, R. R. & Ryther, J. H. 1962. Studies of marine planktonic diatoms. 1. *Cyclotella nana* Hustedt, and *Detonula confervacea* (Cleve) Gran. *Can. J. Microbiol.* 8:229–39.

Hancke, K., Hancke, T. B., Olsen, L. M., Johnsen, G. & Glud, R. 2008. Temperature effects on microalgae photosynthesis-light responses measured by O_2 production, pulse-amplitude-modulated fluorescence, and ^{14}C assimilation. *J. Phycol.* 44:501–14.

Haxo, F. T. 1985. Photosynthetic action spectrum of the coccolithophorid, *Emiliania huxleyi* (Haptophyceae): 19′hexanoyloxyfucoxanthin as antenna pigment. *J. Phycol.* 21:282–7.

Johnsen, G., Prézelin, B. B. & Jovine, R. V. M. 1997. Fluorescence excitation spectra and light utilization in two red tide dinoflagellates. *Limnol. Oceanogr.* 42:1166–77.

Johnsen, G. & Sakshaug, E. 1993. Bio-optical characteristics and photoadaptive responses in toxic and bloomforming dinoflagellates *Gyrodinium aureolum, Gymnodinium galatheanum*, and two strains of *Prorocentrium minimum*. *J. Phycol.* 29:627–42.

Johnsen, G. & Sakshaug, E. 1996. Light harvesting in bloomforming marine phytoplankton: species-specificity and photoacclimation. *Sci. Mar.* 60:47–56.

Johnsen, G. & Sakshaug, E. 2007. Bio-optical characteristics of PSII and PSI in 33 species (13 pigment groups) of marine phytoplankton, and the relevance for pulse-amplitude-modulated and fast-repetition-rate fluorometry. *J. Phycol.* 43:1236–51.

Kolber, Z. & Falkowski, P. G. 1993. Use of active fluorescence to estimate phytoplankton photosynthesis in situ. *Limnol. Oceanogr.* 38:1646–65.

van Kooten, O. & Snel, J. F. H. 1990. The use of chlorophyll fluorescence nomenclature in plant stress physiology. *Photosynth. Res.* 25:147–50.

Kopf, U. & Heinze, J. 1984. 2,7-Bis(diethylamino)phenazoxonium chloride as a quantum counter for emission measurements between 240 and 700 nm. *Anal. Chem.* 56:1931–5.

Kromkamp, J. C., Domin, A., Dubinsky, Z., Lehmann, C. & Schanz, F. 2001. Changes in photosynthetic properties measured by oxygen evolution and variable chlorophyll fluorescence in a simulated entrainment experiment with the cyanobacterium *Planktothrix rubescens*. *Aquat. Sci.* 63:363–82.

Kromkamp, J. C. & Forster, R. M. 2003. The use of variable fluorescence measurements in aquatic ecosystems: difference between multiple and single turnover measuring protocols and suggested terminology. *Eur. J. Phycol.* 38:103–12.

Kroon, B., Prezelin, B. B. & Schofield, O. 1993. Chromatic regulation of quantum yield for photosystem II charge separation, oxygen evolution and carbon fixation in *Heterocapsa pygmaea* (Pyrrophyta). *J. Phycol.* 29:453–62.

Longstaff, B. J., Kildea, T., Runcie, J. W., Cheshire, A., Dennison, W. C., Hurd, C., Kana, T., Raven, J. A. & Larkum, A. W. D. 2002. An in situ study of photosynthetic oxygen exchange and electron transport rate in the marine macroalga *Ulva lactuca* (Chlorophyta). *Photosynth. Res.* 74:281–93.

Ludden, E., Admiraal, W. & Colijn, F. 1985. Cycling of carbon and oxygen in layers of marine microphytes: a simulation model and its eco-physiological implications. *Oceologia* 66:50–9.

MacKinney, G. 1941. Absorption of light by chlorophyll solutions. *J. Biol. Chem.* 140:315–22.

Mitchell, B. G. 1990. Algorithms for determining the absorption coefficient for aquatic particulates using the quantitative filter technique (QFT). *Proc. SPIE Ocean Opt. X* 1302:137–48.

Mitchell, B. G. & Kiefer, D. A. 1988. Chlorophyll *a*-specific absorption and fluorescence excitation spectra for light-limited phytoplankton. *Deep-Sea Res.* 35:639–63.

Morel, A., Lazzara, L. & Gostan, J. 1987. Growth rate and quantum yield time response for a diatom to changing irradiances (energy and color). *Limnol. Oceanogr.* 32:1066–84.

Morris, E. P. & Kromkamp, J. C. 2003. Influence of temperature on the relationship between oxygen- and fluorescence-based estimates of photosynthetic parameters in a marine benthic diatom (*Cylindrotheca closterium*). *Eur. J. Phycol.* 38:133–42.

Mullineuax, C. W. & Allen, J. F. 1988. Fluorescence induction transients indicate dissociation of photosystem II from the bilisome during the state-2 transition in the cyanobacterium *Synechococcus* 6301. *Biochim. Biophys. Acta* 934:96–107.

Neori, A., Vernet, M., Holmhansen, O. & Haxo, F. T. 1988. Comparison of chlorophyll far-red fluorescence excitation spectra with photosynthetic oxygen action spectra for photosystem II in algae. *Mar. Ecol. Prog. Ser.* 44:297–302.

Owens, T. G. 1991. Energy transformation and fluorescence in photosynthesis. *In* Demers, S. [Ed.] *Particle Analysis in Oceanography*. Vol. 27. NATO ASI series G, Springer Verlag, Berlin, pp. 101–37.

Prézelin, B. B., Tilzer, M. M., Schofield, O. & Haese, C. 1991. The control of the production process of phytoplankton by the physical structure of the aquatic environment with special reference to its optical properties. *Aquat. Sci.* 53:136–86.

Revsbech, N. P. 1989. An oxygen microelectrode with guard cathode. *Limnol. Oceanogr.* 34:474–8.

Sakshaug, E., Bricaud, A., Dandonneau, Y., Falkowski, P. G., Kiefer, D. A., Legendre, L., Morel, A., Parslow, J. & Takahashi, M. 1997. Parameters of photosynthesis: definitions, theory and interpretation of results. *J. Plankton Res.* 19:1637–70.

Sakshaug, E. & Holm-Hansen, O. 1977. Chemical composition of *Skeletonema costatum* (Grev) Cleve and *Pavlova* (*Monochrysis*) *lutheri* (Droop) Green as a function of nitrate-limited, phosphate-limited, and iron-limited growth. *J. Exp. Mar. Biol. Ecol.* 29:1–34.

Sakshaug, E., Johnsen, G., Andresen, K. & Vernet, M. 1991. Modeling of light-dependent algal photosynthesis and growth: experiments with the Barents Sea diatoms *Thalassiosira nordenskioeldii* and *Chaetoceros furcellatus*. *Deep-Sea Res.* 38:415–30.

Schofield, O., Prézelin, B. B., Bidigare, R. R. & Smith, R. C. 1993. In situ photosynthetic quantum yield. Correspondence to hydrographic and optical variability within the Southern California Bight. *Mar. Ecol. Prog. Ser.* 93:25–37.

Schreiber, U., Hormann, H., Neubauer, C. & Klughammer, C. 1995. Assessment of photosystem II photochemical quantum yield by chlorophyll fluorescence quenching analysis. *Aust. J. Plant. Physiol.* 22:103–9.

Schreiber, U., Schliwa, U. & Bilger, W. 1986. Continuous recording of photochemical and non-photochemical chlorophyll fluorescence quenching with a new type of modulation fluorometer. *Photosynth. Res.* 10:51–62.

Steemann-Nielsen, E. 1952. The use of radio-carbon (14C) for measuring organic production in the sea. *J. Cons. Int. Explor. Mer.* 18:117–40.

Suggett, D. J., MacIntyre, H. & Geider, R. J. 2004. Evaluation of biophysical and optical determinations of light absorption by photosystem II in phytoplankton. *Limnol. Oceanogr. Methods* 2:316–32.

Webb, W. L., Newton, M. & Starr, D. 1974. Carbon exchange of *Alnus rubra*: a mathematical model. *Oecologia* 17:281–91.

Yentsch, C. S. 1962. Measurement of visible light absorption by particulate matter in the ocean. *Limnol. Oceanogr.* 7:207–17.